PHY479Y Undergraduate Research Project Report: Pattern Evolution in Desiccation Crack Networks

Matthew West

Introduction

Nonequilibrium processes such as drying and cooling in materials can lead to the build up of stresses, causing cracks to form. These processes are widespread in the natural world and are responsible for geophysical pattern formation in crack networks, often on a large scale. Basalt solidifying as it cools can lead to columnar jointing, a geological phenomenon where polygonal prisms of basalt form as a solidification front propagates into the cooling lava. The geometry of these prisms is usually hexagonal, as this is the energetically preferred configuration of cracking caused by the uniform stresses induced across the shrinking surface layer. Columnar jointing can also be seen in tabletop scale experiments; a number of investigations have been undertaken regarding this phenomenon in desiccated corn starch. [1, 2] The first part of my project involved investigating a possible thermal analogue of this system, using coconut oil. A cooling plate was constructed that allowed liquid coconut oil contained in a glass beaker to be cooled from below to temperatures at which it would solidify, which occurs at approximately 25°C. Though cellular patterns were observed, no coherent cracking phenomena occurred. Images of these patterns are presented in Fig. 1.
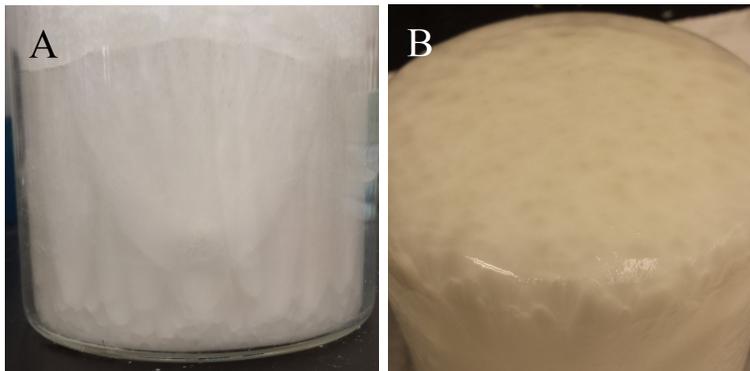

Figure 1: Patterns in coconut oil cooled to a temperature of around 15°C. Pattern formation was more noticeable for coconut oil cooled to higher temperatures, just below its melting point, due to the slower surface contraction for these temperatures. In A, parabolic patterns can be seen where the coconut oil meets the curved face of the cylindrical beaker, increasing in scale as distance from the cooled surface below increases. In B, the underside of the solid coconut oil block can be seen, removed from the beaker. Cellular patterns are observed as a result of solidification, though this is not sufficient to induce cracking.

Owing to similarities between poroelasticity and thermoelasticity, the driving mechanisms behind cracking in columnar jointing are very similar to those in desiccation cracking. However, desiccation cracking often has a rectilinear pattern associated with its crack network. This is due to the hierarchical structure of its crack network, with cracks forming sequentially as the material is cooled. Subsequent cracks tend to join the existing crack network at right-angles, as this corresponds to the fact that normal stress is minimised at a crack surface. Accordingly, stresses parallel to the crack are maximised. As a desiccation crack pattern develops, each crack continually widens, allowing the history of a crack network to be observed by inspection, with the wider cracks in a given network being the oldest.

The rectilinear patterns associated with mud cracking can evolve into hexagonal patterns by a mechanism illustrated in Fig. 2. When the mud is re-wetted, the cracks formed previously in general rejoin, provided the sample is wetted sufficiently. If the mud has a memory of its previous crack network, the lines of previous cracking serve as points of weakness at which the mud will preferentially crack along if allowed to dry again to the point of cracking. As this process is repeated, the order at which established cracks approach a vertex can change, owing to the stochastic nature of crack formation. A crack turning a corner at a vertex tends to round off the right-angle, as this path releases energy most efficiently. If each sequence of the three cracks of a rectilinear 'T' junction arriving at the junction is equally likely, then in time this process averages the junction to a 'Y' junction, with each angle approaching 120°. This evolution from T to Y junctions corresponds to the evolution from a rectilinear to a hexagonal fracture network.

Methods

Experimental Setup

To investigate this evolution, this drying and re-wetting process was repeated experimentally for 152 cycles. A plastic cell of internal dimensions 197x150x12 mm was partially
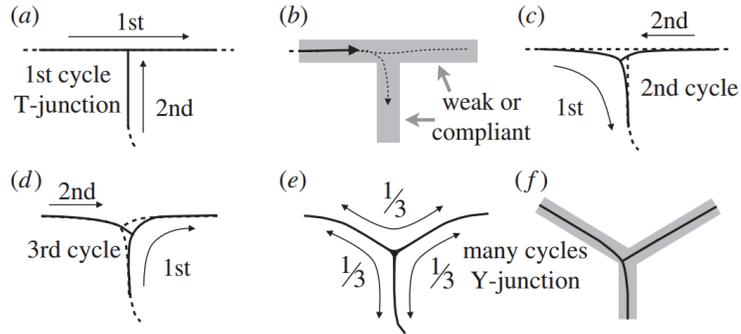
Figure 2: a) An initial T junction forms, and upon wetting and re-drying, b), it is possible for the crack approaching the vertex to turn and c) continue along the secondary line of cracking. This can occur in a different order for subsequent cycles, d), and over time tends to average the T junction to a Y junction. f) Curvature in the vicinity of the vertex usually persists to some extent, however. From Ref. [3]

filled with a slurry of K-bentonite clay, a mixture consisting of approximately 120g of dry bentonite powder and 250g of distilled water. The viscosity of this mixture was similar to water and allowed it to be poured into the cell, forming a uniformly flat surface layer. After the experimental data collection was concluded, the thickness of the sample was measured to be 10.3 ± 0.9 mm, a significantly thicker sample than has been previously investigated for this system. [4] As the length scale of the peds increases with layer thickness, this meant that the corresponding crack network had fewer vertices than would be associated with thinner samples, but was less subject to environmental fluctuations in the topology of the clay surface.

The cell was heated from approximately 50cm above by two 250 W ceramic brooding lamps. This controlled the evaporation and thus shrinkage that, coupled with the adhesion of the sample to the bottom of the cell, caused a reproducible crack pattern to appear. The hot bulbs allowed accelerated evaporation and crack formation, with a single drying cycle taking approximately 2 hours to complete. This allowed for the investigation of a significantly larger number of cycles than was previously possible. Approximately 25,000 images from 152 such cycles were collected over a period of 13 days. The mud could be wetted by
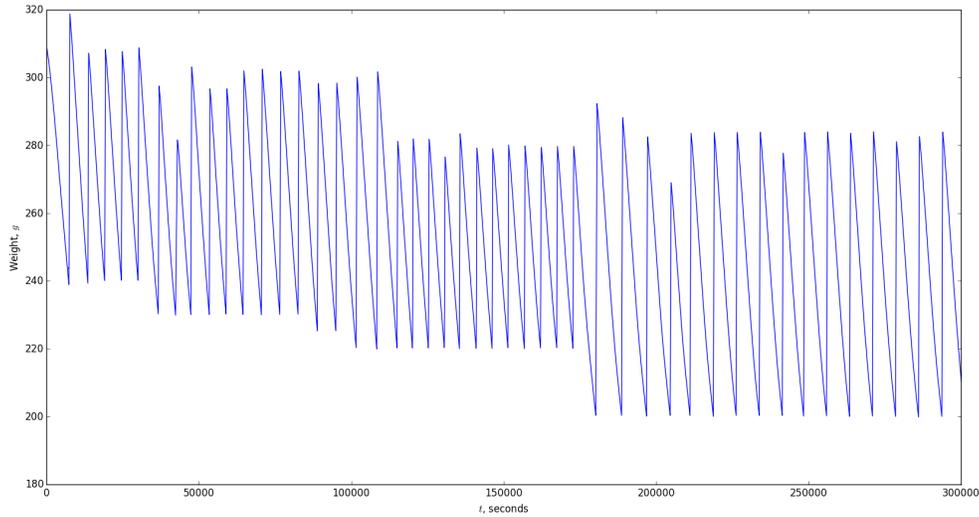
3

Figure 3: A graph showing the variation of weight with time. This corresponds approximately to the first 30 cycles, with the critical wet and dry weights for the cycles beyond this being the same as those for the end of the data visualised. Between peaks the drying is approximately linear, indicating that the material is not being dried completely.

four misting nozzles attached to a pump (150 psi), positioned approximately 15cm above the clay. A Nikon D200 DSLR camera placed directly above the cell took pictures of the mud at equally spaced weight intervals. This, as well as the lighting and wetting, were controlled via a VI created in LABVIEW. An electronic scale upon which the mud cell was placed communicated weight values to the program, turning the lights off and the misters on if the weight value reached below a critical dry weight, decided empirically. This dry weight changed as the topology of the mud surface did, in general requiring a lower weight value to crack completely as the system was iterated. The re-wetting would pulse on for 5 seconds, off for 20 seconds, allowing the dry clay to absorb the water and the cracks to seal while partially mitigating the formation of bubbles in the mud, which negatively interact with pattern formation. The wetting occurred until a certain wet weight was reached, also decided empirically. The variation in time of both the wet and dry weights used in this experiment can be seen in Fig. 3. Once this weight was attained, the misting was turned off by the VI, and the lights back on, allowing a new drying cycle to occur. Pictures were

4

taken and weights were recorded only while the system was drying, a process which was also controlled by the VI, continuously checking the weight reading and taking a picture when it had changed by more than a threshold value. For the majority of the data collected, this threshold was every 0.5g of weight change, but for interesting points in the initial pattern formation, it was lowered to 0.2g.

Image Analysis

For the purposes of investigating the pattern evolution as the system was repeatedly dried and re-wetted, the last picture taken before re-wetting was analysed for each of the 152 cycles. The primary statistic of interest in this evolution is the angles in the crack network at each vertex. In order to extract this information, scripts in MATLAB were used. An initial edge detection was applied to the cropped image, as seen in Fig. 4. This used the *canny* method, as part of MATLAB's *edge()* function. Following this edge detection, the crack network had large areas of noise removed and was skeletonised to just 1 pixel thick, primarily through the use of MATLAB's *bwmorph()* function.

Once a skeletonised image had been created, the vertices at which the crack pattern intersects itself were obtained, again using *bwmorph()*. A circular mesh consisting of two
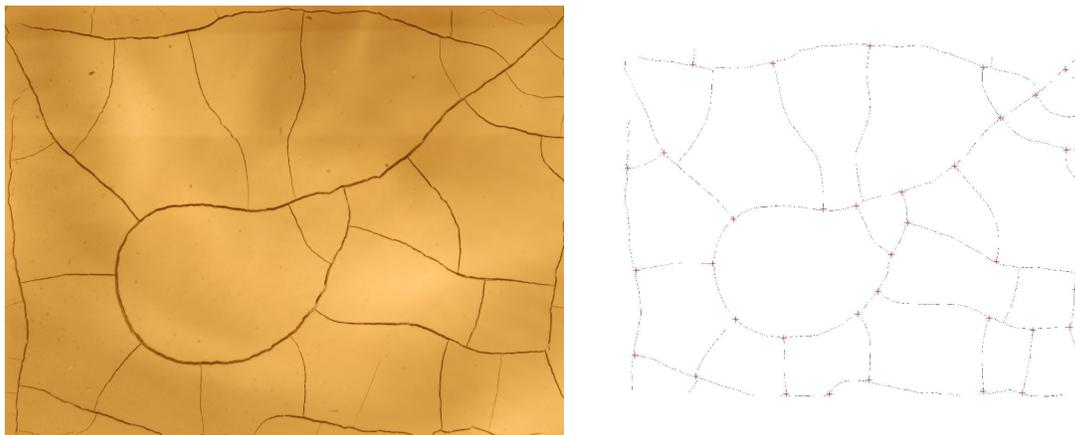

Figure 4: Left: a cropped image of the first crack pattern, just before re-wetting. Right: a skeletonised version of the first crack pattern, with the vertices identified algorithmically and overlayed as red crosses.

concentric rings was used to obtain the angles of the crack network at each vertex. The points where the cracks at each vertex crossed the two rings of the mesh were obtained, with MATLAB's angle function being used to obtain the corresponding angles.

Results and Discussion

A number of things are striking about the pattern evolution observed in the data collected. A departure from the initial rectilinear cracking pattern is clear, with the crack pattern becoming more irregular as the system was iterated. Fig. 5 shows the general features of the pattern evolution at three different stages of the experimental run. It is apparent from Fig. 5 that the crack pattern becomes much less smooth as subsequent drying and wetting occurs; approximately polygonal peds become much less defined. In addition to this, the exposed surface of the mud became much less even, with cratering of the surface in the vicinity of cracks, and air trapped in the wetting process occasionally introducing topological heterogeneities at random points on the surface via bubbling. In general, however, the increased thickness of the sample used mitigated most of the negative effects associated with bubbling. Further issues were presented by the fact that the crack network itself became less complete with some cracks terminating in the centre of a ped, and the cracks themselves became thinner for higher iterations. This made image analysis difficult, though focus on the vertices remained possible without a comprehensive fully-connected crack network being

Figure 5: Left: a cropped image of the third crack pattern, just before re-wetting. Middle: The same pattern after 50 cycles, and right: after 152 cycles.

possible to image for all cycles.

Interesting to note was the formation of the first crack, originating as a straight line in the upper right of the image in Fig. 4, but curving around back on itself to create a loop. This created an atypical central ped larger than the others with a continuously curved surface. The formation of this curved crack could correspond to an anisotropic stress field with a preference to stresses in the radial direction, perhaps induced by memory effects associated with the pouring of the liquid slurry into the plastic cell. Another possible source of this initial crack could be associated with a nonhomogeneous heat distribution from the heat lamps, possibly causing irregular drying in the surface layer of the mud.

Fig. 6 shows the evolution of a single vertex over the first 102 drying cycles. For this vertex, a clear progression from a 90° T junction to a 120° Y junction is apparent. This is in accordance with the process outlined in Fig. 2. A more comprehensive analysis of angle evolution for entire images is possible, with histograms indicating the relative frequency of equally spaced angle bins for a given drying cycle. Fig. 7 shows four such histograms, with angle bins on the horizontal axis, and frequency on the vertical axis. A scatter plot of the histogram data is overlayed with a double-peaked gaussian fit for each value of n, representing the number of drying cycle to which the data corresponds. An evolution is apparent, though not as clear-cut as the progression shown for the vertex in Fig. 6. In general, for rectilinear patterns the expected histogram has a significant peak around 90°, and another approximately half as large at 180°, corresponding to the dominant presence
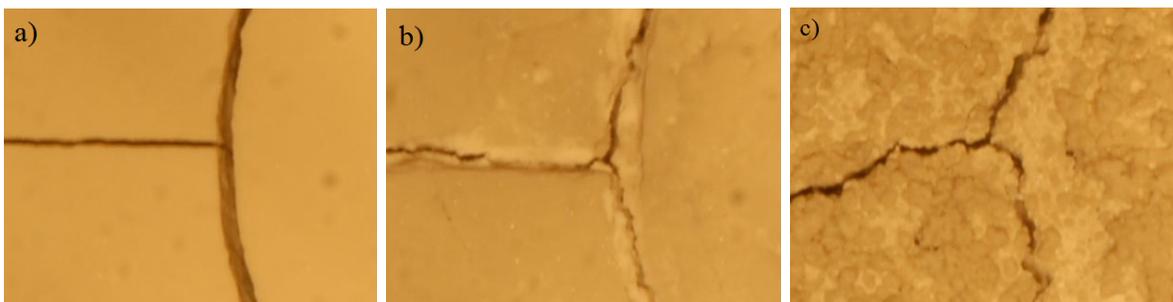

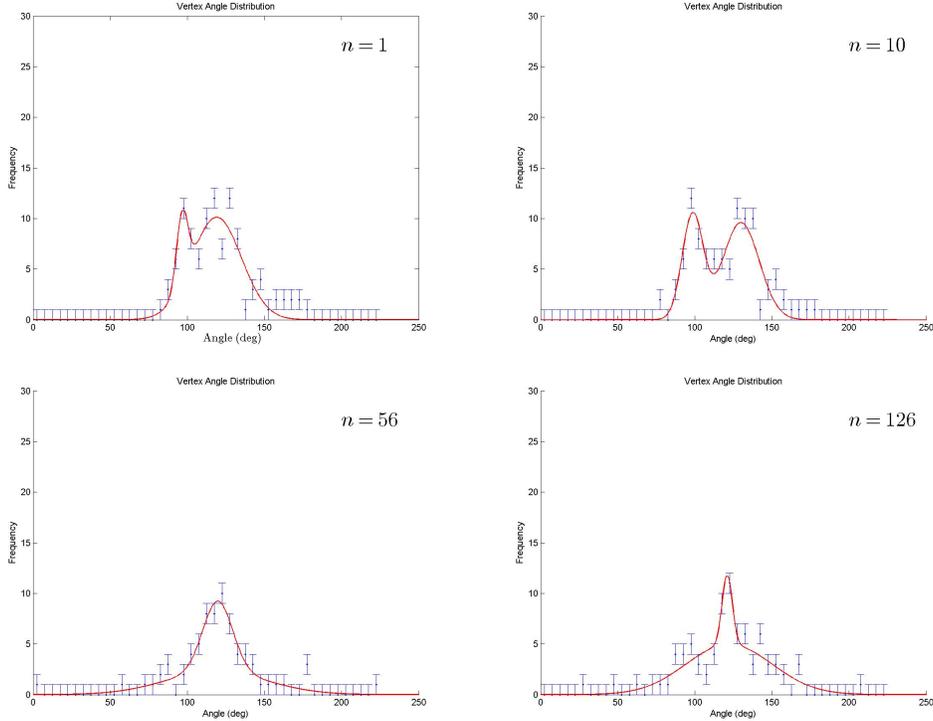Figure 6: Vertex at the middle-left of the curved ped, for a) 1 cycle, b) 29 cycles, and c) 102 cycles.

Figure 7: Histograms showing the relative frequency of angles for each angular interval, for various values of n.

of T junctions. These peaks are visible for $n = 1$ and $n = 10$, and though there is a dip around $120°$ for $n = 10$, approximate Y junctions seem to be present in even the initial crack pattern. At higher crack cycles, there is a clear suppression of $90°$ and $180°$ peaks, with $120°$ emerging as the favoured centre of the angular distribution. Fig. 8 shows the modal angle bin, that is, the angular interval which has the highest frequency for a given drying cycle, plotted as a function of n. After an initial spike, the modal angle quickly approaches $120°$. It is apparent for higher n, particularly above $n = 100$, that the value of the modal angle converges to $120°$, indicating that the histograms for these values of n are centred on $120°$ and vary less about this angle as the system is iterated. This corresponds to a more established crack pattern dominated by Y junctions for higher n.

There are a number of sources of statistical error with respect to identifying vertices and measuring angles in the image analysis. In order to reduce the occurrence of falsely identified vertices, any vertex within a certain threshold distance to a previously identified
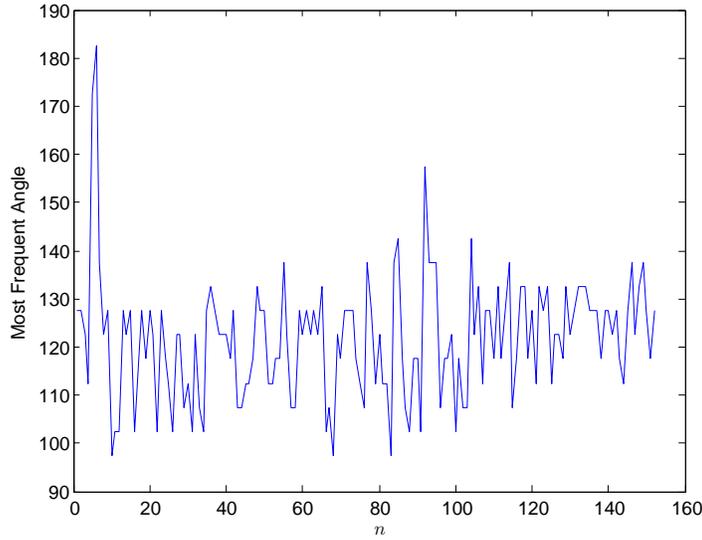
Figure 8: The most frequent angle as a function of crack cycle, n.

vertex was disregarded. This inevitably led to some vertices being ignored that would have otherwise contributed to the statistics. Additionally, any vertex that had more than three cracks converging at it was disregarded in the image analysis.

A further problem in obtaining the angles develops as the crack pattern becomes more crooked. Over small length scales, the path of a crack can diverge quite quickly from what a linear interpretation near the vertex predicts. This leads to significant variation in the values of the angles measured as the size of the circular mesh used to obtain them is varied. It then becomes a matter of interpretation as to what mesh size best represents the perceived angle of the vertex, though a preferential length scale is not always apparent.

A possible issue with the mud sample used is that the large thickness corresponded to the crack pattern having a large ped size, and as such the sample size of eligible vertices was reduced. This was a trade-off for making the crack network more robust to environmental changes on the surface of the mud, such as those associated with the aforementioned cratering and bubbling, allowing the same crack network to be analysed for a significantly larger number of drying and wetting iterations. Further experimental investigation of this system

9

would benefit from increasing the scale of the experiment in the horizontal plane, allowing a thicker sample resilient to random disturbances, together with a larger number of vertices eligible to be analysed. An issue encountered here with thicker samples is that re-wetting a thicker sample can prove challenging. Preliminary runs of data were taken with samples marginally thicker than the one presented here. The initial cracks that widened as the rest of the crack pattern developed proved to be very difficult to reseal, even when completely submerged in water. Submerging the sample in this way can also induce further cratering in the vicinity of the crack, with the edges of the surrounding peds avalanching into the space between them, caused by the increased pressure associated with submersion. This was partially controlled by only allowing the mud to reach a certain dryness such that the crack network did not develop to the extent that any of the cracks were too wide to reseal, and re-wetting the sample over a longer time scale to allow the clay to absorb the water before submersion occurred. Regardless, in many of the early runs for the data presented in this report, it was not possible to entirely reseal some of the wider cracks, though topological evolution of the mud surface seemed to eliminate this problem as the system was iterated, with the wider cracks narrowing over time.

Further heterogeneities were introduced to the mud through the formation of clusters of small protrusions on the surface. This effect was most apparent near the edges of the sample, and could possibly be evidence of some component of the mud being transported to the edges of the cell as the system was dried and re-wetted, and accumulating on the surface. This appears to be a property of the variety of clay used and could perhaps be eliminated by the choice of an alternative substance for any future investigation into this system.

Conclusion

The formation of crack networks in a geophysical context has been described and an experimental investigation into the evolution of a crack pattern in a bentonite sample has

been presented. A layer of K-bentonite 10.3 ± 0.9 mm thick has been iteratively dried and re-wetted for 152 cycles, and the evolution of the crack network characterised. While pattern evolution has been observed to occur, it is far from the robust transition from a rectilinear to a hexagonal crack network that is expected for long time scales. A number of recommendations have been made for further investigation into this type of system, with pattern formation expected to be more robust for thicker samples with a greater horizontal extent, and with an alternative choice of material. Complete pattern evolution may require a time scale far beyond what is practical to reproduce experimentally, though these adjustments would provide an opportunity to investigate this system for longer than has previously been achieved.

Bibliography

[1] Müller, G. *Journal of Geophysical Research: Solid Earth* **103**(B7), 15239–15253 (1998).

[2] Goehring, L. and Morris, S. W. *EPL (Europhysics Letters)* **69**(5), 739 (2005).

[3] Goehring, L. *Philosophical Transactions of the Royal Society of London A: Mathematical, Physical and Engineering Sciences* **371**(2004), 20120353 (2013).

[4] Goehring, L., Conroy, R., Akhter, A., Clegg, W. J., and Routh, A. F. *Soft Matter* **6**(15), 3562–3567 (2010).